Journal of Physics: Conference Series

PAPER • **OPEN ACCESS**

Research on Optimal Control of Dual Active Full-Bridge DCDC Converters

To cite this article: Weichao Shi and Haiyan Zhang 2022 *J. Phys.: Conf. Ser.* **2383** 012063

Research on Optimal Control of Dual Active Full-Bridge DC-DC Converters

Weichao Shi[1a], Haiyan Zhang[2b]

[1,2]School of Electrical Engineering, Shanghai Dianji University, Shanghai, China

[a]email: 2811078679@qq.com , [b]email: zhanghy@sdju.edu.cn

Abstract. The dual active full-bridge (DAB) DC-DC converter is an important module for realizing bidirectional energy transmission. At present, it has been widely used in solid-state transformers, DC microgrids, electric vehicle charging piles and other fields. It can carry out high-capacity transmission, and can electrically insulate the primary and secondary sides, and has a wide range of uses.

1. Introduction

In the converter, there are many kinds of conversion devices capable of bidirectional energy flow, including isolated and non-isolated, and non-isolated, which can only be used in low power consumption occasions[1]. The isolated converter realizes electrical isolation through a high-frequency transformer, and can also realize high-power bidirectional energy transmission. Dual active full-bridge DC-DC converters are widely used and become one of the important core devices in emerging fields such as DC microgrids and electric vehicles. For the selection of control strategies in DAB converters, the most common and widely used one is single-phase shift, single-phase-shift control mode, which has only one degree of freedom, simple operation, and can meet the maximum transmission power. However, when the voltage ratio between the two ends of the converter does not match, the inductor current stress will increase in the circuit. In order to solve this problem, control methods such as extended phase shift, double phase shift, and triple phase shift control are proposed [2-4]. Among them, the extended phase shift and double shift control modes have two degrees of freedom, which can improve the efficiency and at the same time, the operation mode is not too complicated. The triple phase-shifting control method has three degrees of freedom, and the control is relatively complicated, and due to the increase in the number of degrees of freedom, the soft-switching technology of multiple modes is not easy to implement. Therefore, based on the extended phase shift, this paper optimizes the inductor current stress, reduces the ohmic loss, and improves the efficiency.

2. Analysis of the working principle of the converter

2.1. Topology of DAB

The main circuit topology of the DAB converter is shown in Figure 1. The overall structure is symmetrical and consists of two large H-bridge circuits, a high-frequency isolation transformer T, an auxiliary inductance and the sum L of the leakage inductance of the high-frequency transformer [5]. Among them, S_1-S_4 are the four switches of the H-bridge on the primary side, Q_1-Q_4 are the four switches of the H-bridge on the secondary side; V_1 is the input side voltage, V_2 is the output side voltage, iL is the inductor current, C_1 and C_2 are the filter capacitors of the DC source on the input and output sides respectively, V_p is the central output voltage of the left H-bridge, V_s is the terminal voltage on the primary side of the transformer, and the transformation ratio of the high-frequency isolation transformer is n:1. By applying pulses to the eight switch tubes to control the turn-on and turn-off alternately, the direction and magnitude of the transmission power of the converter can be controlled, thereby realizing the bidirectional flow of energy.

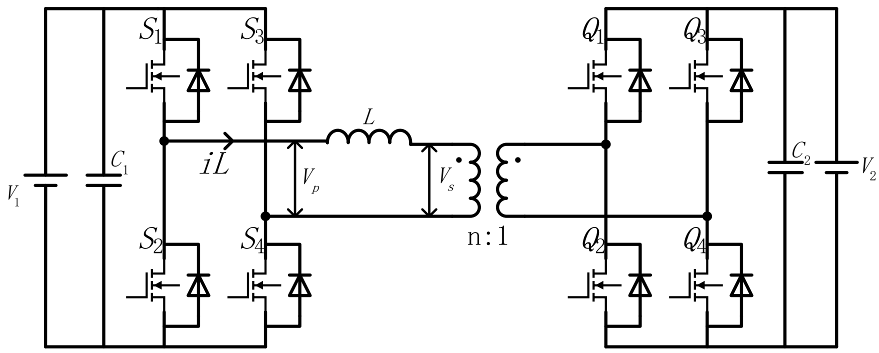

Figure 1. DAB converter topology.

2.2. The Driving Signal of DAB

Under the extended phase-shift control strategy of the DAB converter, the timing waveform diagram of each variable is shown in Figure 2. Where TS is half of the switching period, D_1 is the internal shift of the primary H-bridge, D_2 is Compared to the inter-bridge shift of the two H-bridges. Compared with the single phase-shift control method, the extended phase-shift control method increases the internal shift in the left H-bridge, f is the switching frequency, k is the voltage conversion ratio on both sides of the converter, which is $k = V_1/(nV_2)$. This paper assumes, $k \geq 1, 0 \leq D_2 \leq D_1 \leq 1$

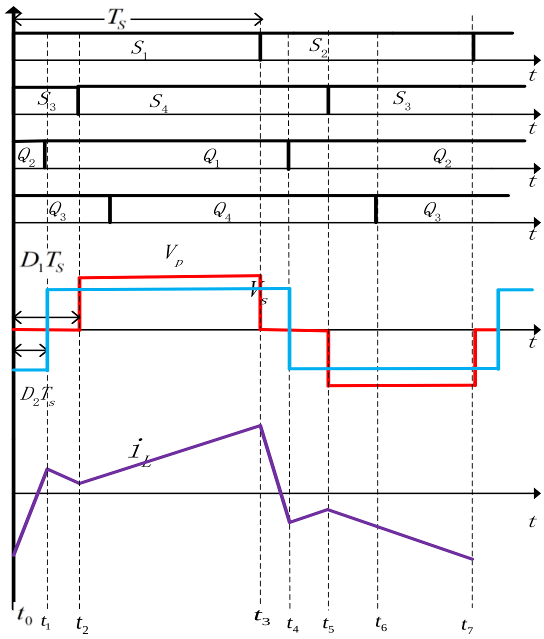

Figure 2. Timing waveform diagram of DAB.

2.3. Mathematical model

After the converter is stable, at the time point marked in Figure 2, the inductor current expression is:

$$\begin{cases} iL(t_0) = -\frac{nV_2}{4fL}[k(1-D_1)+(2D_2-1)] \\ iL(t_1) = \frac{nV_2}{4fL}(kD_1-k+1) \\ iL(t_2) = \frac{nV_2}{4fL}[k(D_1-1)+2D_2-2D_1+1] \\ iL(t_3) = \frac{nV_2}{4fL}[k(1-D_1)+(2D_2-1)] \end{cases} \tag{1}$$

In order to simplify the analysis process of the converter, take the SPS control, the per unit power $P_N = \mathrm{n}V_1V_2(8fL)^{-1}$ is the maximum transmission power, and the power is forwarded. From the average power calculation formula $P = T_S^{-1}V1\int_0^{T_S} iL(t)dt$ .The transmission power formula [6] is:

$$P_0 = \frac{P}{P_N} = 2(D_1^{\ 2} - D_1 - 2D_1D_2 + 2D_2) \tag{2}$$

3. Analysis of the working characteristics of the converter

3.1. Current Stress Characteristics

The inductor current stress refers to the maximum value of the inductor current generated by the DAB converter in a steady state. The magnitude of the current stress has an important impact on the device selection, power loss and stable operation of the circuit. In the operating mode selected in this paper, according to the analysis of the operating characteristics of the inductor current, at the moment of t_4, the peak value of the inductor current appears and reaches the maximum. Also, under SPS control, the current at maximum power $I_N = nV_2(8fL)^{-1}$ is the reference value, at this time, the per-unitized expression of the inductor current stress is:

$$i = \frac{iL}{I_N} = 2[k(1-D_1)+2D_2-1] \tag{3}$$

3.2. Soft switching characteristics

The switching loss of the device also has a great influence on the transmission efficiency of the converter. In order to achieve higher transmission efficiency, the switch device needs to implement soft switching technology. In the operation mode of this paper, in order to realize the ZVS characteristics of the primary side H-bridge switch, it is necessary to meet the $iL(t_1) < 0$.To realize the ZVS characteristics of the secondary side H-bridge switch, it is necessary to meet the $iL(t_3) > 0$.Therefore, the conditions for realizing the ZVS characteristics of all switches are:

$$\begin{cases} D_1 > \frac{k-1}{k} \\ D_2 < \frac{2D_1 - kD_1 + k - 1}{2} \end{cases} \tag{4}$$

4. Optimization of control strategies

4.1. Minimum current stress optimization

In the operating mode selected in this paper, the maximum moment of inductor current occurs at time t4, in order to find the optimal set among many shift-phase combinations, on the basis of the established Lagrange function, this paper adds the inequality relation constraints between shift-phase and switch to realize ZVS characteristics, using the KKT condition method [7], Find the optimal solution. The standard form of this method is:

$$\begin{cases} \min\ Y(X) \\ s.t \quad P_{EPS}(X) - P_0 = 0 \\ \quad\quad B_j(X) \le 0,\ j = 1, 2, \cdots, q \end{cases} \tag{5}$$

Where: Y(X) is the objective function; $P_{EPS}(x)-P_0$ is the equality constraint; $B_j(j=1,2\ldots q)$ is the determined inequality constraint; q represents the number of inequalities. From (5), the equations that satisfy the KKT condition can be listed:

$$\begin{cases} L = 2\left[k(1-D_1) + (2D_2 - 1)\right] + \lambda[2\left(D_1^{\ 2} - D_1 - 2D_1D_2 + 2D_2\right) - P_0] + \\ \mu_1(D_2 - D_1) + \mu_2(D_1 - 1) + \mu_3(1 - k + 2D_2 - 2D_1 + kD_1) + \\ \mu_4(k - 1 - kD_1) + \mu_5(-D_2) \\ \lambda \ne 0, \mu_1, \mu_2, \mu_3, \mu_4, \mu_5 \ge 0, \dfrac{\partial L}{\partial D_1} = 0, \dfrac{\partial L}{\partial D_2} = 0 \\ D_2 - D_1 \le 0, D_1 - 1 \le 0, 1 - k + 2D_2 - 2D_1 + kD_1 \le 0, k - 1 - kD_1 \le 0, -D_2 \le 0 \\ 2\left(D_1^{\ 2} - D_1 - 2D_1D_2 + 2D_2\right) - P_0 = 0 \\ \mu_1(D_2 - D_1) = 0, \mu_2(D_1 - 1) = 0, \mu_3(1 - k + 2D_2 - 2D_1 + kD_1) = 0, \\ \mu_4(k - 1 - kD_1) = 0, \mu_5(-D_2) = 0 \end{cases} \tag{6}$$

Equation (6) is solved to obtain the optimal combined solution for the shift phase, and the expression for the minimum inductor current stress per unit:

$$\begin{cases} D_1 = 1 - \sqrt{\dfrac{P_0}{2(k-1)}} \\ D_2 = \dfrac{2-k}{2}[1 - \sqrt{\dfrac{P_0}{2(k-1)}}] + \dfrac{k-1}{2} \end{cases}$$
$$i = 4(k-1)\sqrt{\dfrac{P_0}{2(k-1)}} \tag{7}$$

Due to the conditional limitation of the relationship between D_1 and D_2, the range of the obtained shift ratio D_1 and the corresponding transmission power P_0 are:

$$\begin{cases} \dfrac{k-1}{k} < D_1 \le \dfrac{3k-3}{3k-2} \\ \dfrac{3k-3}{(3k-2)^2} \le P_0 < \dfrac{2k-2}{k^2} \end{cases} \tag{8}$$

Under the condition of given transmission power P_0 and voltage transformation ratio k, the optimal shift ratio combination D_1 and D_2 of the DAB converter can be obtained from this.

4.2. Minimum Current Stress Control Algorithm

The control method of minimum current stress is shown in Figure 3. The closed-loop control method is given in the figure. On the one hand, by sampling the output voltage V_2 and comparing it with the given output voltage V_{ref}, the error is sent to the PI adjustment controller, and the real-time transmission power P_0 is output; On the other hand, the output voltage and input voltage are obtained by sampling, and the conversion ratio k of the real-time voltage is further obtained, and then P_0 and k are sent to the optimized control algorithm to obtain the optimal shift ratio combination D_1, D_2, and finally ,D_1, D_2 are feed into the driver module of the DAB converter.

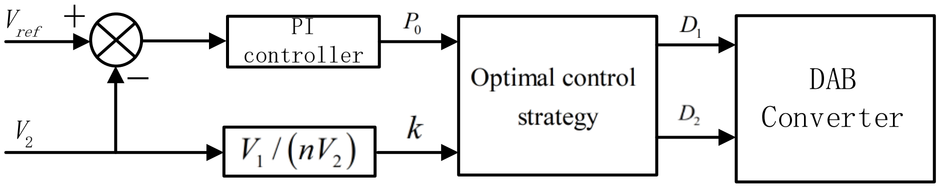

Figure 3. Modulation strategy control block diagram.

5. Footnotes

Finally, in order to verify the accuracy and effectiveness of the optimal control scheme proposed in this paper, a DAB converter simulation model is built through MATLAB/Simulink, and the simulation parameters are shown in Table 1.

Table 1. Parameters of The DAB Model.

Parameter	Value
Input Voltage V_1	300V
Output Voltage V_2	100V
Inductance L	200uH
Turns Ratio n	2
Input Capacitor C_1	1000uF
Output Capacitor C_2	1000uF
Switching Frequency f	20kHz

When the output voltage is 100V (k=1.5) and the output power is 500W, the figure shows the trend of the voltage across the inductor and the current waveform flowing through it under the single phase-shift control method and the optimal extended phase-shift control method. It can be shown from the figure that the peak inductor current of the EPS after optimal control, compared with the traditional phase-shift control method, the stress of the inductor current is significantly reduced, which is consistent with the theoretical analysis. Figure 5 shows the currents flowing through the switches S_1, S_4, and Q_1 and the voltage waveforms at both ends. It can be seen that the ZVS characteristic of zero-voltage turn-on at both ends of the switches has been effectively realized.

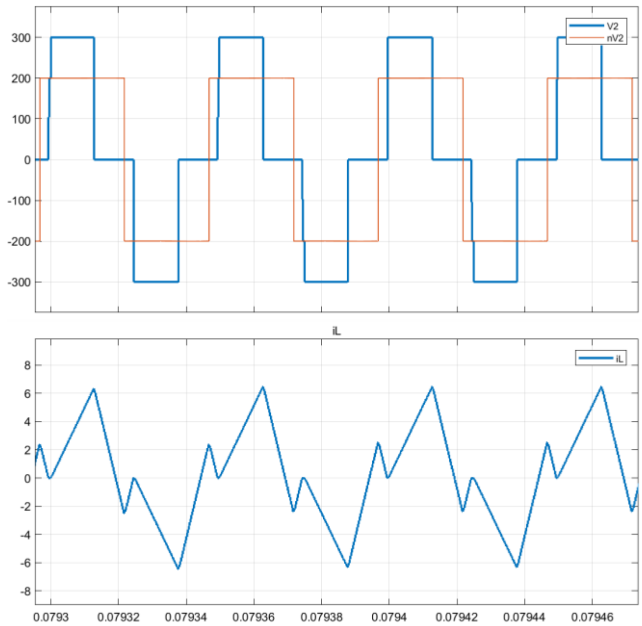

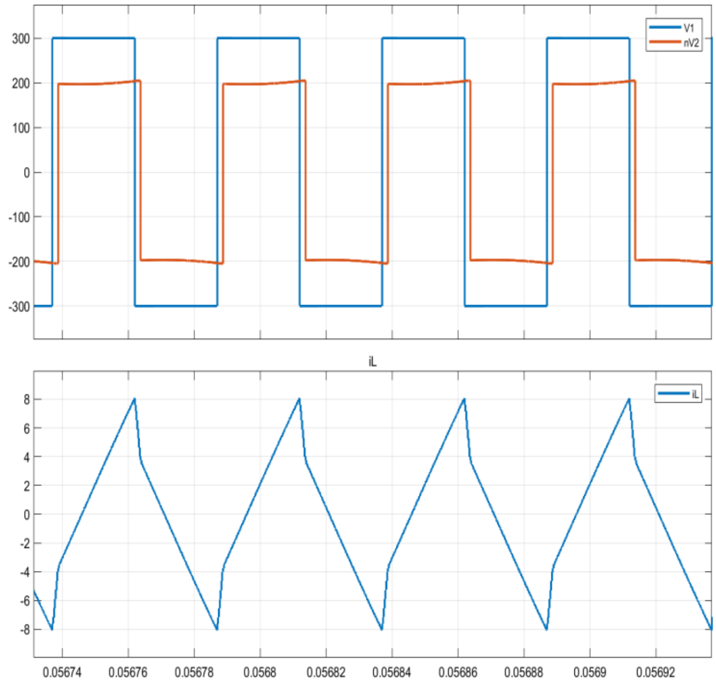

Figure 4. SPS (left) and Optimized EPS (right).

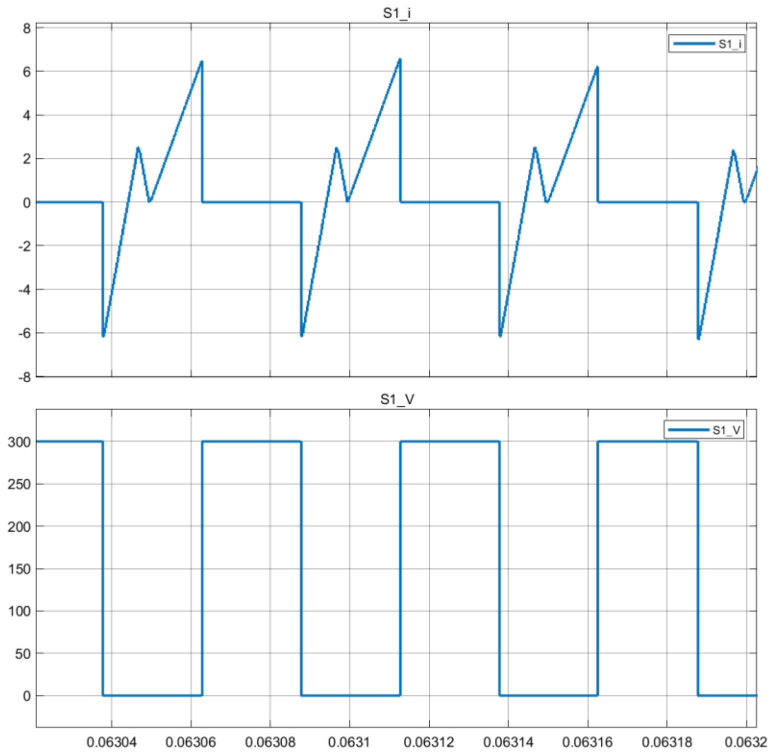

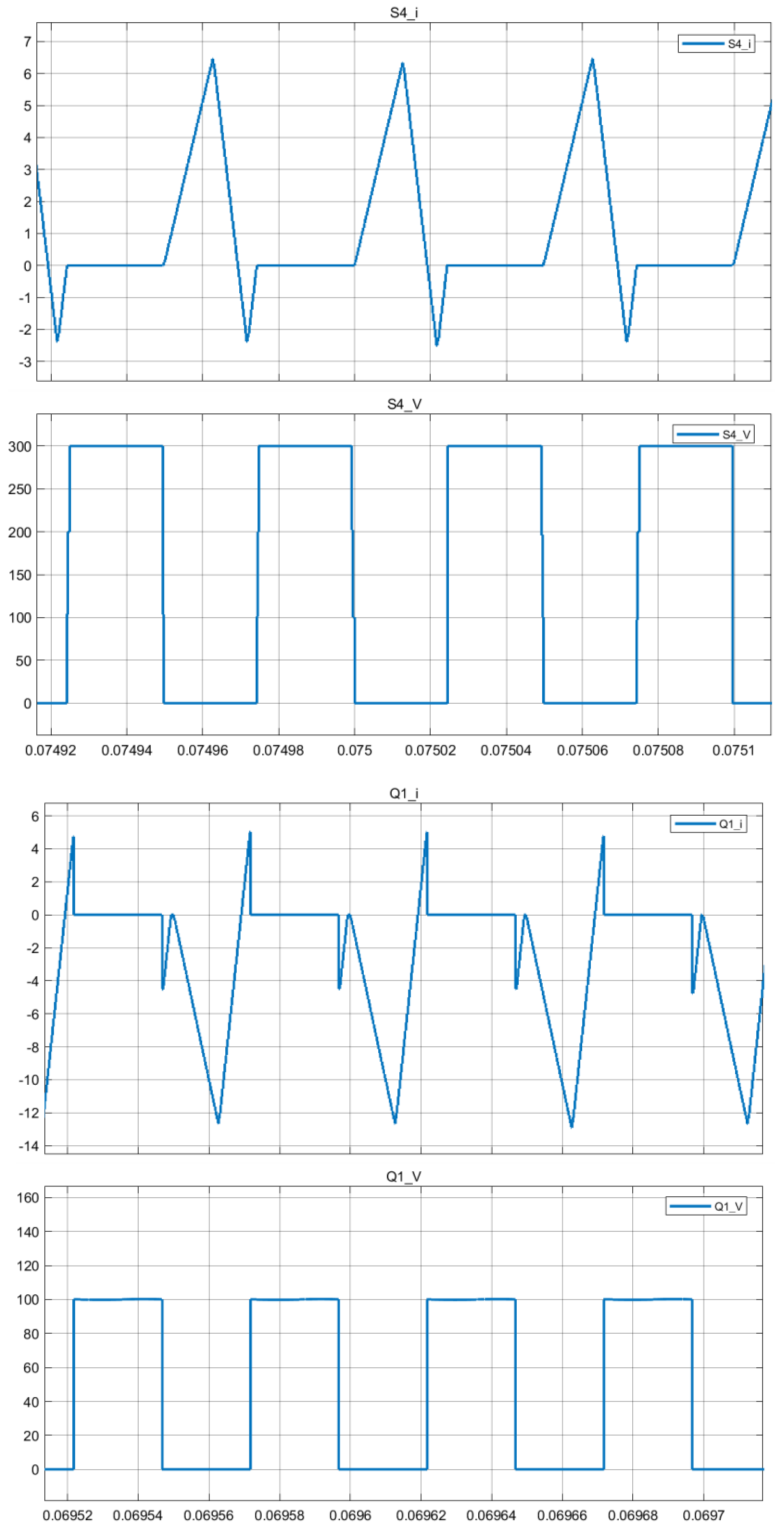

Figure 5. Switch waveform.

6. Conclusion

In this paper, through the analysis of the DAB converter under the extended phase-shift control strategy, the mathematical model of the inductor current and transmission power is obtained, and through the

Lagrange multiplier method and the KKT condition, an optimal control of the inductor current is obtained. The optimal combination of the trajectory and the shift phase can simultaneously satisfy the zero-voltage turn-on of all switches in the full power range. Theoretical analysis and simulation results show that when the voltage ratio at both ends of the converter does not match, compared with the single phase-shift control method, the optimized control method proposed in this paper can further reduce the inductor current stress and achieve ZVS of all switches. characteristics to improve the transmission efficiency of the converter. Secondly, the control method proposed in this paper has strong portability, and does not need to introduce too many circuit parameters in the implementation process of the control strategy.

References

[1] Zhao B, Song Q and Liu W 2014 IEEE Transactions on Power Electronics. **29**: 4091-06.
[2] Zhou J, Wang H and Zhang J 2020 Proceedings of the CSEE. **40**: 3990-4003.
[3] Zhao B, Song Q and Liu W 2013 IEEE Transactions on Industrial Electronics **60**: 4458-67.
[4] Zhao B, Yu Q and Sun W 2012 IEEE Transactions on Power Electronics. **27**: 4667-80.
[5] Hu S, Li X D and Bhat A K S 2019 IEEE Transactions on Power Electronics. pp 904-15.
[6] Shao S, Jiang M M and Ye W W 2019 IEEE Transactions on Power Electronics. pp 10193-205.
[7] Huang J, Wang Y and Li Z Q 2016 IEEE Transactions on Power Electronics. pp 4169-79.